RECEIVED
JAN 25 1995
OSTI

CONF-9510221--2

NARCOTICS DETECTION USING FAST-NEUTRON INTERROGATION

Bradley J. Micklich and Charles L. Fink
Technology Development Division
Argonne National Laboratory
9700 South Cass Avenue, Argonne, IL 60439
(708) 252-4849 / Fax: (708) 252-1774

ABSTRACT

Fast-neutron interrogation techniques are being investigated for detection of narcotics in luggage and cargo containers. This paper discusses two different fast-neutron techniques. The first uses a pulsed accelerator or sealed-tube source to produce monoenergetic fast neutrons. Gamma rays characteristic of carbon and oxygen are detected and the elemental densities determined. Spatial localization is accomplished by either time of flight or collimators. This technique is suitable for examination of large containers because of the good penetration of the fast neutrons and the low attenuation of the high-energy gamma rays. The second technique uses an accelerator to produce nanosecond pulsed beams of deuterons that strike a target to produce a pulsed beam of neutrons with a continuum of energies. Elemental distributions are obtained by measuring the neutron spectrum after the source neutrons pass through the items being interrogated. Spatial variation of elemental densities is obtained by tomographic reconstruction of projection data obtained for three to five angles and relatively low (2 cm) resolution. This technique is best suited for examination of luggage or small containers with average neutron transmissions greater than about 0.01. Analytic and Monte-Carlo models are being used to investigate the operational characteristics and limitations of both techniques.

1. Introduction

Fast-neutron interrogation techniques are being studied for the detection of illicit substances (e.g., narcotics) in luggage and cargo containers. X-ray techniques are also being considered, but they often have problems detecting narcotics in background materials which are of similar density and atomic number. Fast-neutron based techniques are attractive because they offer the possibility of determining the densities of light elements such as carbon, nitrogen, and oxygen within individual volume elements. Narcotics are composed primarily of these elements, but are relatively poor in nitrogen and oxygen and relatively rich in carbon and hydrogen than most other substances likely to be found in legitimate cargo.

This paper discusses two different fast-neutron techniques. The first technique is based on detecting gamma rays from fast-neutron interactions with the material being interrogated. Volumetric elemental densities are determined by analyzing the characteristic gamma rays emitted from the material. We discuss the variant of the technique referred to as Pulsed Fast-Neutron Analysis (PFNA) being developed by Science Applications International Corporation [1]. This technique is suitable for examination of large containers because of the good penetration of the fast neutrons and the low attenuation of the high-energy gamma rays. The second technique, Fast-Neutron Transmission Spectroscopy (FNTS), is based on measuring the neutron spectrum from a continuum energy neutron source after

The submitted manuscript has been authored by a contractor of the U. S. Government under contract No. W-31-109-ENG-38. Accordingly, the U. S. Government retains a nonexclusive, royalty-free license to publish or reproduce the published form of this contribution, or allow others to do so, for U. S. Government purposes.

DISTRIBUTION OF THIS DOCUMENT IS UNLIMITED

MASTER

the neutrons have passed through the items to be interrogated. The basic technique was first examined [2] for bulk material analysis, and is best suited for examination of luggage or small containers having an average transmission ratio greater than about 0.01.

2. Pulsed Fast-Neutron Analysis

Pulsed Fast-Neutron Analysis uses nanosecond pulses of monoenergetic neutrons produced by accelerating deuterons onto a deuterium gas target. The neutron beam is scanned vertically across the cargo container by a movable collimator. Scanning along the length of the container is accomplished by moving the container horizontally. Depth information is obtained using time-of-flight between the accelerator pulse and the arrival of a gamma ray in NaI detectors located outside the container. Since the neutrons produced have velocities of about 4 cm/ns, the accelerator pulse must be at most a few ns if the voxel depth (thickness) is to be about 10 cm. In luggage or smaller containers, where higher resolution may be required for explosives detection, the minimum pixel dimension along the beam is about 5 cm, since the practical minimum pulse width is about 1.25 ns. The 4.44-MeV gamma from the first excited state in ^{12}C and the 6.13-MeV gamma ray from the second excited state in ^{16}O are used to generate a qualifier that indicates the presence of narcotics.

2.1 PFNA signal estimates

The gamma-ray signal detected in a PFNA inspection system depends sensitively on the incident neutron energy used, since the inelastic scattering cross sections are strong functions of energy. Neutron energies greater than 6.5 MeV are required to detect ^{16}O, with the inelastic scattering cross sections being largest between 8.2 and 8.25 MeV (requiring a deuteron energy of about 5.5 MeV). However, since the inelastic scattering cross sections vary rapidly in this energy range, the energy distribution of the source neutrons must be well-known and stable so that the effective or spectrum-averaged cross sections remain constant.

The PFNA geometry shown in Figure 1 was modeled with the radiation transport code MCNP [3] to estimate the signal at various detector locations for

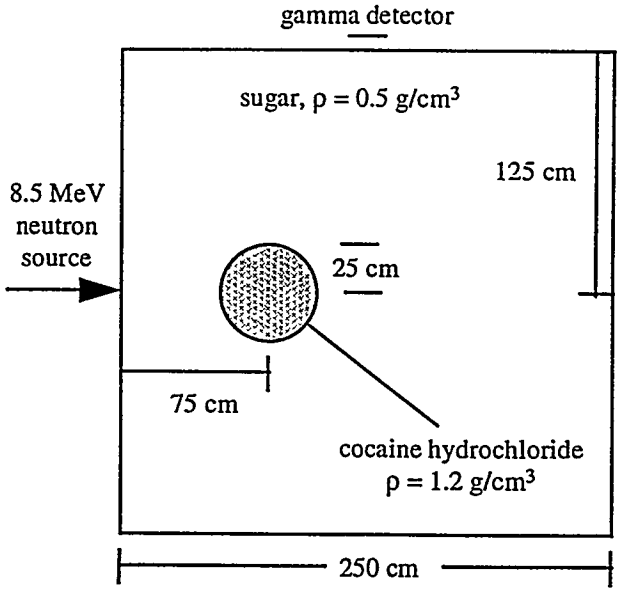

Figure 1. Schematic of PFNA geometry used in MCNP simulations.

typical PFNA neutron beam parameters and a variety of container loadings. The background materials and densities considered were: sugar (0.5 g/cm^3); coffee (0.74 g/cm3); iron/plastic (0.5 g/cm^3); and iron (0.15 g/cm^3). For each background material, the model was run with and without a 25-cm radius sphere of cocaine hydrochloride ($C_{17}H_{21}NO_4$-HCl, 1.2 g/cm^3) centered 75 cm from the front face. The gamma rays per source neutron reaching detectors at the top center and the center back of the container are shown in Figure 2 for the sugar background. Examination of these curves indicates that at a position of about z = 50 cm there are clearly changes in the carbon and oxygen atom density. Also, the total mass density increases in the cocaine case, since the gamma-ray generation rate falls off more quickly with distance into the container. However, comparison of the count rates shown in Fig. 2(a) and 2(c) indicate that we cannot perform a simple addition of counts from detectors located in different positions. Similar results are seen for the other container background materials.

The gamma-ray signal as a function of time at a certain detector location can be transformed into information about elemental densities inside the container as

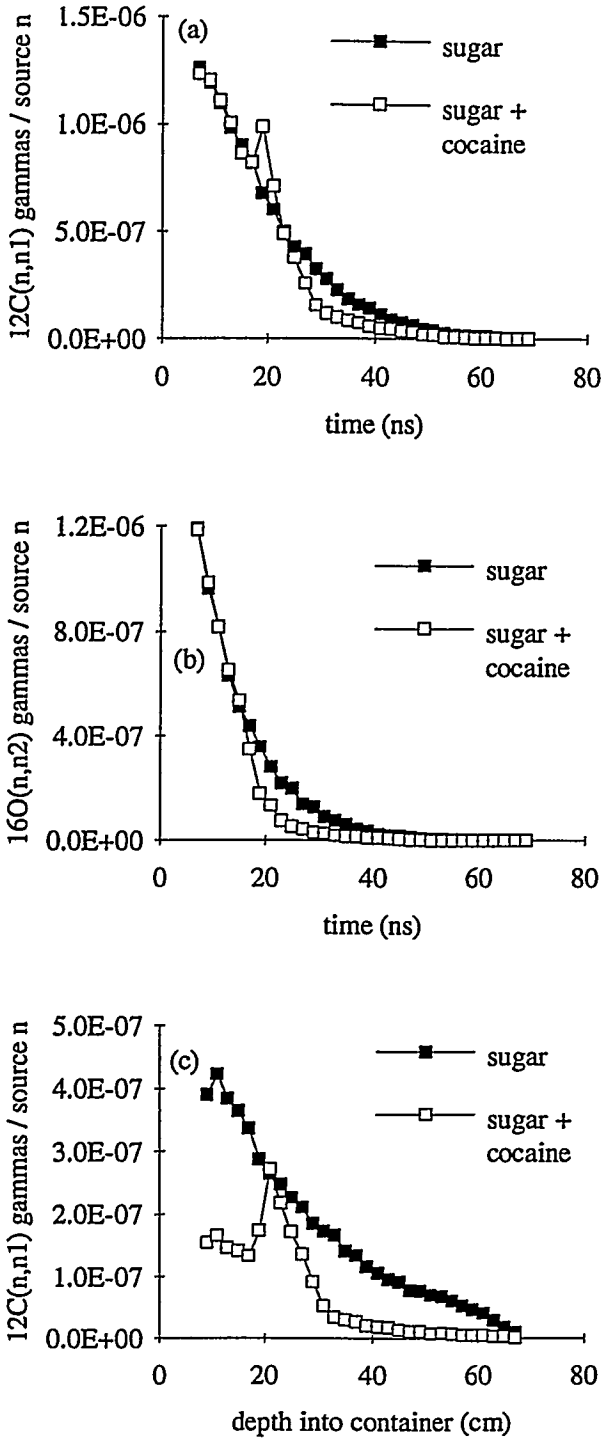

Fig. 2. Results of MCNP PFNA simulations: (a) ^{12}C gammas at center top detector, (b) ^{16}O gammas at center top detector, (c) ^{12}C gammas at rear detector.

a function of position using the equations

$$n_c(t_i) = S_c(t_i) / \left[e^{-\lambda z_i} (V\sigma_c) \left(A_d / 4\pi r_i^2 \right) e^{-\mu_c r_i} \right]$$
$$n_o(t_i) = S_o(t_i) / \left[e^{-\lambda z_i} (V\sigma_o) \left(A_d / 4\pi r_i^2 \right) e^{-\mu_o r_i} \right] \quad (1)$$

where n_c (n_o) = carbon (oxygen) atom density
S_C (S_O) = 4.44-MeV (6.13-MeV) gamma count rate
z_i = depth into container
λ = fast-neutron attenuation constant
V = volume of voxel
σ_C (σ_O) = carbon (oxygen) inelastic cross section
A_d = detector area
r_i = voxel-detector distance
μ_C (μ_O) = 4.44-MeV (6.13-MeV) gamma attenuation constant

This model corresponds to a phenomenological model of gamma-ray generation and transport described in [4], and makes the simplifying assumption that gamma rays caused by scattered neutrons are unimportant. To determine n_c and n_o we would have to know the details of the container contents, because we need to know λ, μ_c and μ_o. (where λ is the fast-neutron attenuation constant and μ_c and μ_o are the attenuation coefficients for the carbon and oxygen gamma rays, respectively) as functions of position throughout the container. However, instead of determining densities directly, one might detect cocaine based on the ratio of concentrations C/O. The ratio n_c/n_o can be written as

$$\frac{n_c}{n_o} = \frac{S_c(t_i) \cdot \sigma_o}{S_o(t_i) \cdot \sigma_c} \cdot e^{(\mu_c - \mu_o) r_i} . \quad (2)$$

If the details of the cargo loading are not known, one can (to first order) ignore the difference in attenuation between the carbon and oxygen gamma rays, but this will lead to a larger uncertainty in the resulting C/O ratio.

2.2 Count rates for PFNA inspection systems

The count rate for a PFNA system can be written as

$$R = \{\langle T_n\rangle \langle T_\gamma\rangle\}[S_n I_p \tau_p f \Delta\Omega_n]\{S_\gamma \Omega_\gamma\}\langle\varepsilon_\gamma\rangle \quad (3)$$

where R = detector count rate
$\langle T_n\rangle$ = average neutron transmission to voxel
$\langle T_\gamma\rangle$ = average gamma transmission to detector
S_n = zero-degree neutron emission (n/sr-s-μA)
$\Delta\Omega_n$ = voxel solid angle from neutron source
I_p = peak accelerator current (μA)
τ_p = pulse time width (s)
f = accelerator pulse repetition rate (1/s)
S_γ = gamma source (gammas/sr-n)
Ω_γ = solid angle of detector from voxel
$\langle\varepsilon_\gamma\rangle$ = average gamma-ray detector efficiency

Using the count rates per source neutron shown in Figure 2, the actual count rates (Table 2) are obtained by multiplying by the estimated neutron source rates and gamma detection efficiency. For a deuteron energy of 5.5 MeV, an average beam current of 100 μA, and a 2-atm gas target 5 cm thick, the number of neutrons incident on the region defined by the cocaine sphere is $2.4\cdot10^{10}\cdot\Delta\Omega_n\cdot\langle\varepsilon_\gamma\rangle$. Assuming that the sphere occupies a solid angle of 0.026 sr and that the gamma-ray detection efficiency is 0.2, with a sugar background we obtain count rates of 85 and 45 cps for the C and O lines in the sugar background, and 124 and 22 cps for the C and O lines with the cocaine sphere. Results for the other background materials are obtained in a similar manner.

The required number of counts to detect the difference in the C/O ratios in sugar and cocaine will depend on the background and on the accuracy to which we need to know the ratio. If we assume a signal-to-background ratio of one, and a 20% accuracy in determining the C/O ratio, then we will need approximately 300 counts in the $^{16}O(n,n2)$ peak for the cocaine case. This implies a counting time of 300/22 = 14 s per voxel for the sugar-loaded container, or about 75 minutes per side for a 40-ft container (assuming that the voxels are about 1 ft^3). This time can be shortened by using more detectors to increase the count rate. For less dense loadings, like the iron-filled container, inspection times will be much faster because the smaller attenuation allows more neutron and gamma penetration so that the entire container can be scanned in a single pass. Assuming the same accelerator and target parameters as for the sugar container, we get a counting time of 300/225 = 1.33 seconds per voxel, or a total time of 7 minutes for a 40-ft container.

2.3 Other fast-neutron cargo inspection concepts

Other similar concepts for container inspection have been proposed [5,6]. The concept proposed by GammaMetrics uses a microsecond-pulsed d-t neutron source and collimated detectors. Another interesting

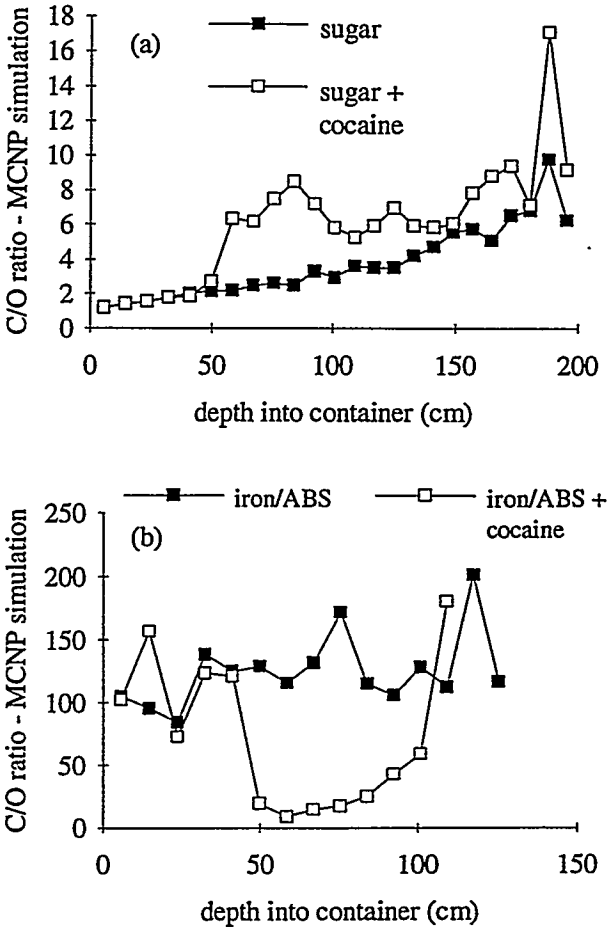

Figure 3. Carbon-to-oxygen ratio as a function of position in container for backgrounds consisting of (a) sugar and (b) iron and ABS plastic.

possibility would be a combination of the SAIC and GammaMetrics concepts, which would use collimated detectors and a long-pulse (μsec) or continuous d-d source. This would have the benefits of detectors which would look directly at a voxel of interest (and hence be relatively insensitive to gamma rays created by scattered neutrons) and of higher count rates. The accelerator would also have a much simpler pulse-forming network than required for nsec pulsing.

3. Fast-Neutron Transmission Spectroscopy

Fast-Neutron Transmission Spectroscopy (FNTS) uses standard time-of-flight (TOF) techniques to measure the energy spectrum of neutrons emitted from a collimated continuum source before and after transmission through an interrogated sample. The energy spectrum of the transmitted neutrons depends on the integrated density of the elements present in the line-of-sight from the neutron source to the detector and on the total cross sections of those elements. A schematic drawing of a typical FNTS system is shown in Figure 4. The collimator may define a pencil beam which obtains information about one projection line-of-sight (one pixel) at a time, or may define a fan beam which allows the interrogation of a line of pixels simultaneously if a linear detector array is used. The areal densities (atoms/cm^2) for individual elements are obtained by a linear least-squares unfolding of the transmission spectrum using the total cross sections for the elements of interest [7].

3.1 Monte-Carlo simulations

The Monte Carlo radiation transport code MCNP was used to simulate neutron transmission through a number of phantoms containing bulk shapes of narcotics. A simple three-body phantom containing bulk narcotics is shown in Figure 5(a). The simulations assumed a parallel beam of neutrons irradiating a slice of the phantom, corresponding to a fan-beam geometry. The neutron source is the ^{9}Be(d,n) reaction at E_d = 5 MeV. This deuteron energy results in a source with high neutron yield in the range 1-4 MeV, which contains many resolved resonances for the light elements. Analog transport was used (i.e., no variance reduction) so that each neutron from the source represents one neutron from a real source. The number of neutron histories run ($1.4 \cdot 10^6$ per pixel) was chosen to simulate a one-second exposure for a maximum count rate of 10^5/s in any given detector at an average transmission of 0.5. The transmission data are unfolded using a linear least-squares routine to determine the elemental areal densities, which are then fed into the tomographic reconstruction routines described below.

3.2 Contraband detection algorithms

In the FNTS technique, each detector measures the energy-dependent transmission along a particular line of sight through the object of interest. This neutron transmission spectrum can be unfolded to obtain the elemental density integrated along the line-of-sight of the detector. A radiographic image for the unfolded element at a given orientation of the suitcase relative to the detector system is then produced by combining the data from all of the detectors. These radiographic images of the elemental areal densities can provide useful information in detecting the presence or absence of illicit substances. In practice, however, the overlap ping of the elemental distributions from spatially separated objects introduces a significant number of false positives (indication of narcotics when none are present) and false negatives (failure to detect narcotics when present). This is especially true considering that the resolution of the radiographic images produced by a FNTS system will be relatively poor.

Table 2. PFNA count rates for background and background + cocaine calculated with MCNP.

	^{12}C(n,n1)	^{16}O(n,n2)
sugar (0.5 g/cm^3)	85	45
sugar + cocaine	124	22
coffee (0.74 g/cm^3)	17	10
coffee + cocaine	22	4.4
iron/plastic (0.5 g/cm^3)	150	1.5
iron/plastic + cocaine	187	25
iron (0.15 g/cm^3)	49	15
iron + cocaine	1620	225

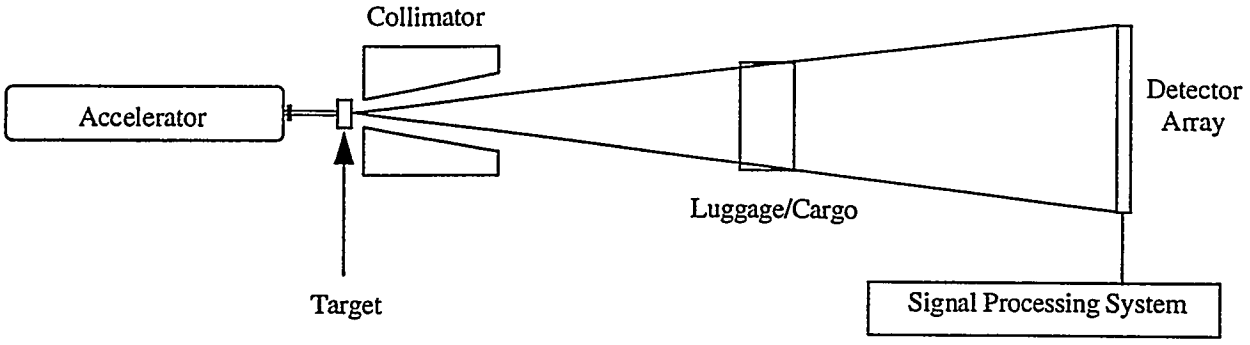

Figure 4. Schematic drawing of a Fast-Neutron Transmission Spectroscopy (FNTS) system.

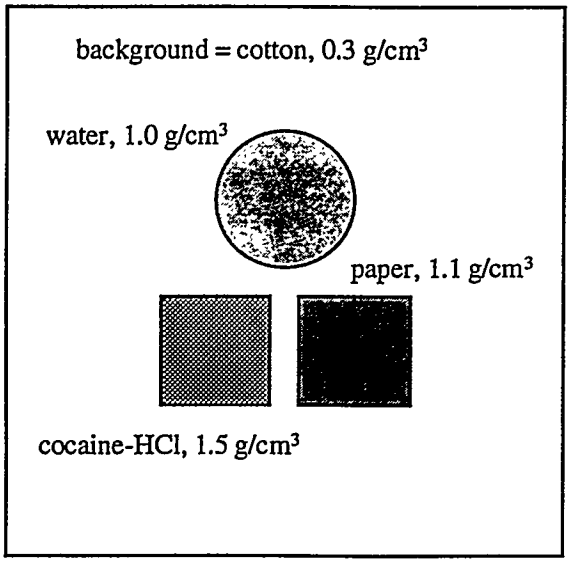

Figure 5. Schematic of the three-body phantom used for drug detection example with FNTS.

We are working in three areas to develop techniques to reduce the number of false positives and false negatives. In the first area, we are using tomographic reconstruction techniques to provide spatial separation of the objects.[8] In reconstruction for medical applications, the goal is to provide an accurate high-resolution visual image. In our case, the goal is more limited and consists of providing sufficient spatial separation between objects to decrease the number of false positives and false negatives. This more limited objective allows us to reduce the number of projections and to use relatively coarse projection resolution to meet system requirements on the length of time available for a particular scan.

In our initial investigations we have kept the number of projections to 7 or fewer and limited projection resolution to 0.5 to 2 cm. We have also kept the pixel resolution equal to the projection resolution, although recent work has investigated the use of pixel resolutions smaller than the projection resolution. Most of the MCNP modeling was done used a 2-cm projection resolution, and the images were reconstructed using a pixel resolution of 2 cm. We have used the algebraic reconstruction technique of maximum likelihood developed for emission spectroscopy. [9] While the number of iterations can be a parameter in the construction, we have kept the number fixed at 25. Initial surveys found that the reconstruction technique and the number of iterations did not have a significant impact on the final results. This could change as we optimize various parameters and include realistic noise distributions.

The second area of investigation involves the development of better signatures for indicating the presence or absence of contraband materials. Here the term "signature" is used to represent some combination of the measured elemental densities that indicates the presence of a contraband material. The measured data from a pixel will consist of elemental densities that are due to various contributions of contraband and benign materials. Some of this material will actually be located within the pixel of interest and some will be due to artifacts from the tomographic reconstruction process. There will also be statistical uncertainties in the

elemental data due to the finite number of counts detected and to the unfolding process. The goal in this second area is to develop a contraband signature that maximizes the differences between contraband and benign materials given the measured uncertainties. The development of this contraband signature is complicated because the functional relationships between measured elemental densities do not have to be linear, contraband materials of interest often have a wide range of densities and compositions, and benign materials of interest cover a wide range of materials and densities that are not well characterized. An example of this is in detection of explosives in luggage. In this case there is a wide range of explosive densities and compositions as well as a large number of benign objects that are not well characterized in terms of compositions.

In our initial evaluation of tomographic reconstruction techniques, we have used a relatively simple contraband signature, which we refer to as the equivalent contraband density signature. After reconstruction, there will be associated with each voxel a measured mass density ρ_i^{meas} for each of the unfolded elements (i). For each compound (j) that we are interested in detecting, we have an associated mass fraction $m_f^j(i)$ for each element in the compound. If we divide the measured density ρ_i^{meas} by the mass fraction $m_f^j(i)$, then the result is the postulated density of compound j in the voxel. If the voxel contained only compound j, then for each element we would calculate the same compound j density for the voxel. If the voxel contains a combination of compound j and other materials, then the resulting densities for the jth compound will differ. The density of compound j possible in the voxel would be the smallest compound density calculated based on individual elements. For example, the equivalent contraband density ρ_j can be defined for narcotics as

$$\rho_j = smallest\ of \left[\frac{\rho_H^{meas}}{m_f^j(H)}, \frac{\rho_C^{meas}}{m_f^j(C)}, \frac{\rho_O^{meas}}{m_f^j(O)} \right].$$

In this expression we have ignored the fact that narcotics could contain small quantities of nitrogen and chlorine. This is because the uncertainties we have observed in unfolding these elemental densities is about the same size as the relatively small concentrations of these elements in the narcotics considered. If the accuracy can be improved, then these elements could easily be added to the definition of the equivalent contraband density. If more than one contraband material is of interest, we calculate the equivalent contraband density for each material of interest and then use the largest equivalent density. For drugs we considered cocaine hydrochloride, cocaine, heroin hydrochloride, and heroin. The main advantage of the equivalent contraband density signature is that the derived density will always be greater than or equal to the actual contraband density present in that voxel. The disadvantage is that many benign materials will yield a nonzero contraband density signature and, therefore, lead to an increase in the number of false positives.

The third area in which we are exploring different algorithms is image processing. The tomographic reconstruction, combined with a particular contraband signature, provides a two-dimensional density image of a slice of the interrogated object. In this image, pixels with large values are more likely to contain contraband than those with small values. The object is to develop algorithms that will automatically process this image and predict the presence or absence of a contraband object. This process of determining the presence or absence of a particular object within an image is an active area of research in the field of image processing. For these preliminary studies, however, we simply divide the measured equivalent contraband density into four density regions, set all pixels within a particular region to the same density, and visually inspect the resulting image. We also determine the amount of contraband material within each region and compare it to the amount actually present.

Figure 6 shows the 3 and 5 angle reconstructions of the bulk narcotics phantom of Fig. 5. The left two images show the equivalent contraband signature. The right two images show the results of applying three different thresholds (0.3, 0.6, and 0.9 g/cm^3) to the equivalent contraband image. The container size is 40

cm and the pixel and projection resolution are 2 cm. The projection areal density data were obtained by direct integration of the Fig. 5 phantom with no measurement or unfolding errors added. The threshold images show that an equivalent contraband density threshold of 0.9 g/cm^3 is sufficient to detect the presence of the cocaine without detection of the other objects. As this threshold is lowered the other objects begin to falsely indicate the presence contraband. Qualitatively, the five-angle projection is better than the three-angle projection although the improvement is relatively small.

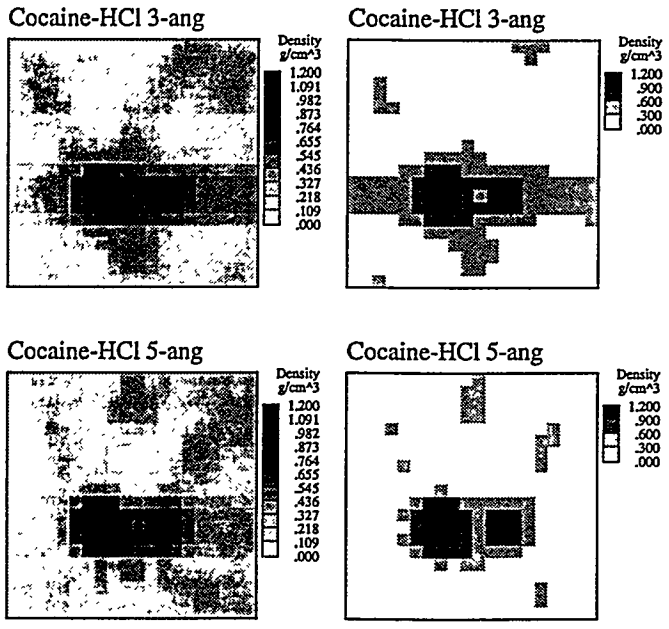

Fig. 6. Equivalent contraband density images for the phantom of Fig. 5. The exact projection data with no errors were used in the reconstructions.

Figure 7 shows the same phantom with the same number of projections, but the elemental projection data are the unfolded areal densities obtained from MCNP transmission simulations. In general, the results are equivalent to those obtained using the actual projection data. This indicates that errors from the statistical uncertainties and from the unfolding algorithms have not introduced significant uncertainties into the projection data.

We have also looked at the effects of mixing various benign materials with the contraband. Figure 8 shows several reconstructed threshold images of mixtures of cocaine and sugar using 3 and 5 projections. The images on the left of Fig. 8 correspond to the reconstructed image in which the contraband contains pure cocaine. The images on the right correspond to a contraband consisting of a 50% mixture by weight of cocaine and sugar. The exact areal projection densities with no errors were used in all of the calculations. In this example, five projections does a better job of separating out the cocaine/sugar mixture although there is still some separation for the 3-angle case.

3.3 Systems Studies

MCNP is also used to perform systems studies which can help determine the parameters necessary for a FNTS system to detect narcotics or explosives. The figure of merit used in these system studies is the error in the elemental areal density, since it has been previously shown that the simulated results are scattered about the true result over a range approximately equal to the reported error.[6] Since the errors in elemental

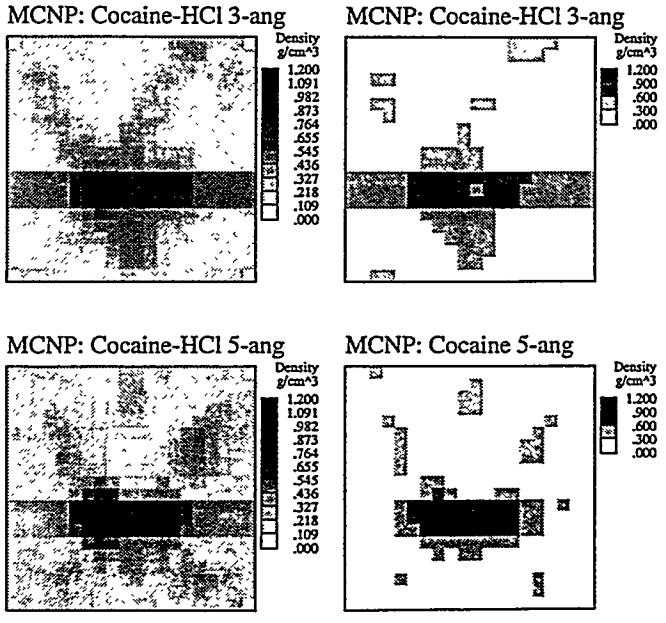

Figure 7. Reconstructed images using projection data obtained from MCNP simulations.

densities depend on the unfolding method and the cross sections, and not on the identity of the sample [10], these systems studies can be performed using any sample (i.e., the results do not depend on what material or combination of materials has been used for the sample). Generally, RDX high explosive has been used as samples for the systems studies.

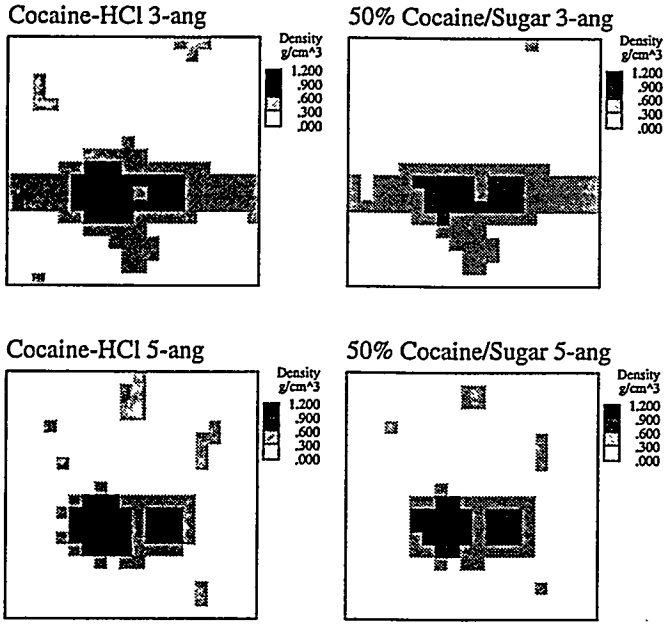

Fig. 8. Threshold images of a 50% mixture of cocaine and sugar by weight.

One example of such a study is presented here, the determination of optimum deuteron beam energy for a ^{9}Be(d,n) source. We have simulated neutron transmission through RDX samples using the neutron source spectrum [11] for deuteron energies between 2.6 MeV and 7.0 MeV. The results for the elemental densities of hydrogen, carbon, nitrogen, and oxygen, and their uncertainties, are shown as functions of incident deuteron energy in Figure 9. These results show that there is little dependence of the errors on incident deuteron energy for $E_d \geq 4.0$ MeV, but that the error in carbon increases rapidly for deuteron energies below that level. Since we assume that carbon detection is important to the detection of narcotics, we may be limited to a minimum deuteron energy of about 4 MeV.

The advantage of using a lower deuteron energy is that the accelerator can be of lower energy, and thus smaller. However, in order to detect the same number of neutrons, the accelerator current would have to be higher, since the neutron yield is lower at lower deuteron energies and since the transmission will be lower for the softer source spectrum. The principal advantage of using higher deuteron energy is thus not to have lower elemental uncertainties but lower accelerator current. While a lower deuteron energy is desirable from the point of view of cost and size, we may find that the need for a greater neutron yield may drive us to consider higher deuteron energies because the current required for lower energies may not be available. As a basis of comparison, Argonne's Tandem Dynamitron at the Fast Neutron Generator facility (now decommissioned) routinely ran with average currents of several microamperes and the pulse structure required for an FNTS system. Accelerator requirements for FNTS are discussed more fully in [12].

4. Concluding Remarks

The use of fast-neutron techniques for detection of illicit drugs appears very promising for both large and small containers. Simulation studies of the PFNA technique for large cargo containers indicates that the PFNA system has the capability to detect 25 kg quantities of drugs. The studies indicate that the amount of time required to scan a particular container will vary depending on whether the container is lightly or heavily loaded. For lightly loaded systems, the scan times are short enough to meet reasonable facility requirements. For heavily loaded systems, however, the scan times need to be significantly reduced. The next level of modeling work should center on exploring methods of reducing the required scanning times. Possible solutions are higher current accelerators, improved gamma detectors using scintillators other than NaI, and the development of a modified PFNA technique using a collimator system. The cost and footprint of a PFNA system are also large and system studies should also be done to determine the best methods of minimizing these parameters.

The use of FNTS for detection of illicit drugs in small containers appears to be very promising. There

still needs to be systems studies performed to find the optimum tradeoffs between system performance and systems size and cost. If such a system were installed for explosive detection, it would require little if any modifications to inspect for illicit drugs.

5. References

1. D. R. Brown, R Loveman, J. Bendahan, and M. Schulze, "Cargo Inspection System Based on Pulsed Fast-Neutron Analysis," *Proc. Int'l Symp. on Contraband And Cargo Inspection Technology*, 235-241, Washington, DC (Oct. 1992).
2. J. C. Overley, "Determination of H, C, N, O, Content of Bulk Materials from Neutron-Attenuation Measurements," *J. Appl. Radiat. Isot.* **36**, 185-191 (1985); "Element-Sensitive Computed Tomography with Fast Neutrons," *Nucl. Instr. Meth. Phys. Res.* **B24/25**, 1058-1062 (1987).
3. J. Briesemeister, ed., "MCNP - A Generalized Monte Carlo Code for Neutron and Photon Transport, Version 3A," LA-7396-M, Rev. 2, Los Alamos National Laboratory (Sept. 1986).
4. B. J. Micklich, C. L. Fink, and T. J. Yule, "Key Research Issues in the Pulsed Fast-Neutron Analysis Technique for Cargo Inspection", SPIE **2276**, 310-320, San Diego, CA (1994).
5. M. J. Hurwitz, R. C. Smith, W. P. Noronha, and K.-C. Tran, "Detection of Illicit Drugs in Cargo Containers Using Pulsed Fast Neutron Analysis," *Proc. Int'l Symp. on Contraband and Cargo Inspection Technology*, Washington, DC (Oct. 1992).
6. E. Rhodes and C. W. Peters, "APSTNG: Neutron Interrogation for Detection of Drugs and Other Contraband," *Proc. Int'l Symp. on Contraband and Cargo Inspection Technology*, Washington, DC (Oct. 1992).
7. B. J. Micklich, M. K. Harper, A. H. Novick, and D. L. Smith, "Illicit Substance Detection Using Fast-Neutron Transmission Spectroscopy," *Nucl. Instr. Meth. Phys. Res.* **A353**, 646-649 (1994).
8. C. L. Fink, B. J. Micklich, T. J. Yule, P. Humm, L. Sagalovsky, and M. M. Martin, "Evaluation of Neutron Techniques for Illicit Substance Detection," *Nucl. Instr. Meth.* **B99**, 748-752 (1995).

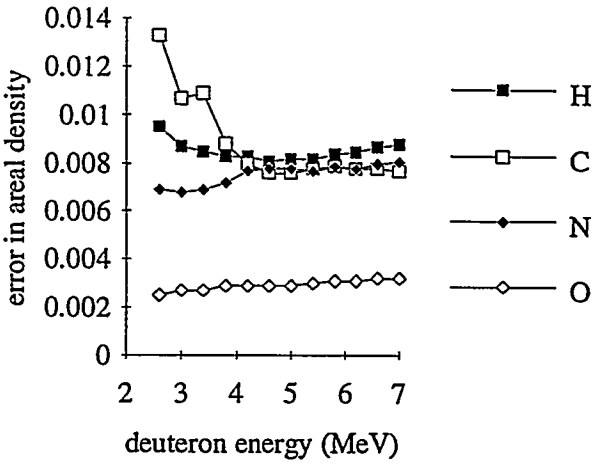

Fig. 9. Variation in errors in areal density of H, C, N, and O versus incident deuteron energy for ^{9}Be(d,n) source (3 cm thick RDX sample).

9. K. Lange and R. Carson, "EM Reconstruction Algorithms for Emission and Transmission Tomography," *J. Comput. Assisted Tomogr.* **8**, 306-316 (1984).
10. Micklich, B. J., C. L. Fink, and L. Sagalovsky, "Transport Simulation and Image Reconstruction for Fast-Neutron Detection of Explosives and Narcotics," European Symposium on Optics for Environmental and Public Safety, Munich, Germany (June 1995).
11. J. W. Meadows, "The Thick-Target ^{9}Be(d,n) Neutron Spectra for Deuteron Energies Between 2.6 and 7.0 MeV," ANL/NDM-124 (Nov. 1991); *Nucl Instr. Meth. Phys. Res.* **A324**, 239-246 (1993).
12. B. J. Micklich, C. L. Fink, and T. J. Yule, "Accelerator Requirements for Fast-Neutron Interrogation of Luggage and Cargo," 1995 Particle Accelerator Conference, Dallas, Texas (May 1995).

6. Acknowledgments

This work was sponsored by the Office of National Drug Control Policy, Counterdrug Technology Assessment Center under contract 6-CO-160-00-195 and by the Federal Aviation Administration Technical Center under contract DTFA03-03-X-00021.

DISCLAIMER

This report was prepared as an account of work sponsored by an agency of the United States Government. Neither the United States Government nor any agency thereof, nor any of their employees, makes any warranty, express or implied, or assumes any legal liability or responsibility for the accuracy, completeness, or usefulness of any information, apparatus, product, or process disclosed, or represents that its use would not infringe privately owned rights. Reference herein to any specific commercial product, process, or service by trade name, trademark, manufacturer, or otherwise does not necessarily constitute or imply its endorsement, recommendation, or favoring by the United States Government or any agency thereof. The views and opinions of authors expressed herein do not necessarily state or reflect those of the United States Government or any agency thereof.